JOURNAL OF GEOPHYSICAL RESEARCH, VOL. 89, NO. B13, PAGES 11,303–11,316, DECEMBER 10, 1984

The Thickness of the Continental Lithosphere

W. R. PELTIER

Department of Physics, University of Toronto

Two independent sets of geophysical data are shown to be particularly sensitive to the thickness of the continental lithosphere. Both are connected with the response of the planet to the last deglaciation event of the current ice age. The first set of data consists of relative sea level histories in the age range 0–10 kyr B.P. from sites along the eastern seaboard of North America. Such data appear to require a continental lithospheric thickness in excess of 200 km. The second set of data consists of the ILS record of the motion of the rotation pole over the time range 0–75 years B.P., which reveals a secular drift at the rate of 0.95 ($\pm$0.15) deg/10^6 years toward Hudson Bay. When the viscosity profile of the mantle is fixed to that required to explain free air gravity and relative sea level data from within the ice margin and the observed nontidal acceleration of planetary rotation, then these observations also suggest a continental lithospheric thickness of the same order.

1. INTRODUCTION

It is well known that lithospheric thickness is an earth property that exhibits strong lateral heterogeneity. The reason for the thickness heterogeneity of oceanic lithosphere is easily understood to be a consequence of the temperature dependence of viscosity. If, by the word lithosphere, we mean the region near the surface of the planet in which the steady state shear viscosity is effectively infinite, then we can understand the observed thickness variations on a very straightforward basis. Since the oceanic lithosphere is an intrinsic part of the large-scale convective circulation of the mantle [*Peltier*, 1980], it follows from the thermal boundary layer nature of this high Rayleigh number flow that boundary layer thickness and thus lithospheric thickness should increase as the square root of ocean floor age [*Peltier*, 1981*a*; *Jarvis and Peltier*, 1982]. It is the exponential dependence of viscosity upon temperature that ensures that the thickness of the thermal boundary layer and the thickness of the lithosphere are closely connected.

The prediction of the theory of thermal convection, that lithospheric thickness should increase as the square root of the age of the seafloor, is rather precisely borne out by the observations. Indeed, the fact that a relatively simple model of thermal convection can also reconcile the observed variations of heat flow and bathymetry, subject only to the assumption that the oceanic lithosphere is to be interpreted as the thermal boundary layer of the large-scale flow in the mantle, is striking testimony to the success of the convection hypothesis itself [*Peltier*, 1980; *Jarvis and Peltier*, 1982]. The hypothesized direct link between the oceanic lithosphere and the mantle general circulation, which is so nicely compatible with the observations, provides a much more compelling explanatory famework than that embodied in plate models [e.g., *Parsons and Sclater*, 1977], since it does not beg the question as to why the plates move.

Our knowledge that the thickness of oceanic lithosphere (LO) does increase as the square root of seafloor age is based upon several different lines of evidence. For example, studies of surface wave dispersion and attenuation across oceanic paths [e.g., *Forsyth*, 1975; *Canas and Mitchel*, 1978; *Canas et al.*, 1980] show that the thickness of the near-surface region, in which wave speeds are high and attenuation is low, exhibits just this age dependence. It has also proven possible to estimate the age dependence of LO by studying the flexural response of the seafloor to surface loads associated with seamounts and with oceanic islands, like Hawaii. This method is different from the seismological method, which infers LO by measuring the depth to a low-velocity high-attenuation zone, but leads to qualitatively similar results. The model that has usually been employed to invert the flexure data is that employed by *Walcott* [1970*a*], which consists of a thin elastic plate over an inviscid substratum. Analyses summarized by *Watts and Daley* [1981] show that the data also require that LO increase as the square root of seafloor age, although the inferred thicknesses are systematically less than the seismic thicknesses by about a factor of 2. This discrepancy is normally attributed to a strong dependence of the apparent thickness upon the age of the load used to make the measurement. The ultimate reason for the reduced thickness observed flexurally is that on the time scale over which seamount loads have been applied, the lower part of the lithosphere has experienced viscous relaxation. A third kind of information that has provided a useful constraint on the variation of LO consists of magnetotelluric data taken with ocean bottom magnetometers on seafloor of various ages. The summary by *Oldenburg* [1980] shows that these data require the presence of a subsurface high-conductivity layer, presumably associated with locally high temperatures and some partial melting, which is in beautiful accord with expectations based upon models of thermal convection at high Rayleigh number [*Peltier and Jarvis*, 1982]. The depth to the good conductor increases roughly as the square root of sea floor age, and the conductivity contrast decreases, presumably on account of a decrease of the fraction of melt. These electrical data fit the seismological picture very well. In summary, then, the observed lateral heterogeneity of the thickness of oceanic lithosphere is strong but reasonably well understood.

Unfortunately, the same level of understanding cannot be claimed with respect to continental lithosphere. The current lack of concensus concerning the thickness of continental lithosphere (LC) is at least in part due to the fact that surface wave seismological data are of little use in these regions. There is little support in surface wave dispersion and attenuation measurements from continental paths for the existence of any subsurface low-velocity and high-attenuation zone. Since LO was inferred seismologically as the observed depth to such a zone, the same seismic method is not readily applicable to the measurement of LC.

Paper number 4B0703.
0148-0227/84/004B-0703$05.00

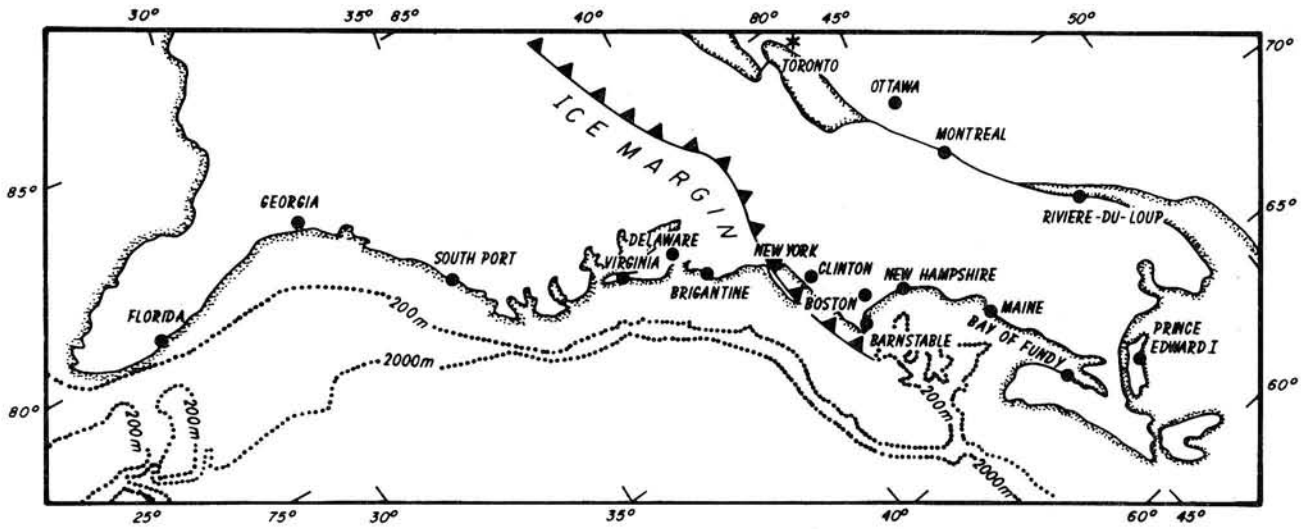

Fig. 1. Location map for sites along the eastern seaboard of North America from which radiocarbon controlled relative sea level histories are available.

In order to infer LC we are obliged to employ other information, and there are several sources to which we can appeal. The first consists of heat flow observations, which when used in conjunction with supplementary data (heat source distributions) can be employed to infer the magnitude of this parameter. Using this source of information, *Sclater et al.* [1980] obtained a continental lithospheric thickness near 120 km, which is approximately equal to the thickness of old oceanic lithosphere. Another line of argument, based upon petrological and body wave seismological considerations, has led *Jordan* [1981] to conclude that the thickness of continental lithosphere was in excess of 250 km. This is sufficiently different from the estimate of *Sclater et al.* [1980] that we might reasonably inquire as to which is nearest the truth. A recent reanalysis of the heat flow data by *Davies and Strebeck* [1982] tends to reinforce the plausibility of the thick lithosphere model preferred by Jordan but cannot be construed as requiring it.

The third technique that has been employed to measure LC makes use of the response of the earth to surface loading. The loads that have most often been employed for this purpose are those applied by the continental ice sheets that existed on Canada and Scandinavia during the last glacial maximum about 18,000 years ago. One of the first measurements of LC using the observed crustal response to these loads was that by *McConnell* [1968], whose analysis of *Sauramo*'s [1958] shoreline data from Fennoscandia led him to suggest a continental lithospheric thickness near 120 km, i.e., the same as that suggested by *Sclater et al.*'s [1980] analysis of the heat flow data. A similar attempt to measure LC was made by *Walcott* [1970*b*, *c*], who analyzed flexure data from the margin of the Laurentide ice sheet and also obtained LC $\simeq$ 120 km. Except for the anomalously thin lithosphere that has been found for the high heat flow Basin and Range Province through analysis of the isostatic response to loading of the crust by Pleistocene Lake Bonneville [*Wu and Peltier*, 1982], it would therefore appear that most data require LC $\simeq$ 120 km and imply that the value preferred by *Jordan* [1981] is implausible.

There are, however, good reasons to doubt the validity of inferences of continental lithospheric thickness that have been obtained through previous analyses of glacial isostatic adjustment. The validity of the inference by *McConnell* [1968], for example, is hard to accept because the data that he employed consisted entirely of strandline information from sites within the ice margin. Theoretical analyses of the sort to be discussed in this paper show, however, that such data may not depend strongly on lithospheric thickness. Only at sites that are immediately external to a load whose scale is as large as the Laurentian ice sheet does the response depend strongly on LC (see section 3 of this paper). For a load of Fennoscandian scale, however, the realization at interior sites does not depend on LC. *Walcott*'s [1970*b*, *c*] analyses are similarly open to question. His inference of continental lithospheric thickness was based upon strandline data from proglacial lakes Agassiz and Algonquin. What Walcott did was to assume that the response at such sites near the ice margin would be in isostatic equilibrium, and he used a steady state flexure model consisting of a thin elastic plate over an inviscid substratum to invert the strandline data for the flexural parameter and thus for lithospheric thickness. This is the same model as was later employed to infer LO from seamount data. Rigorous calculations of isostatic adjustment reported by *Wu and Peltier* [1982], however, do not support the hypothesis that the response near the ice margin is in equilibrium and therefore

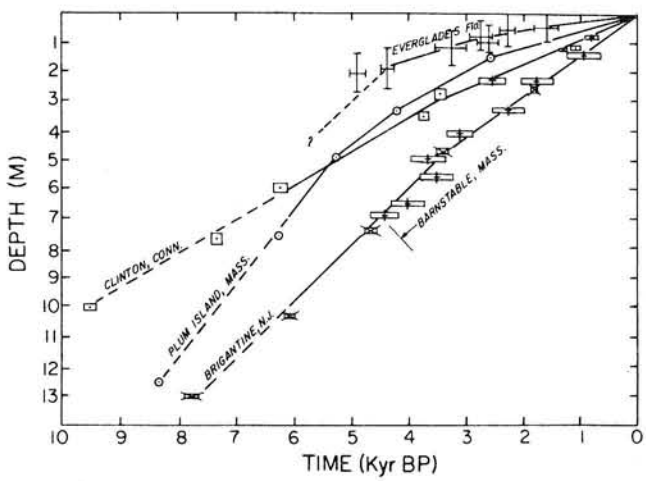

Fig. 2. Relative sea level data from several of the sites located in Figure 1. This figure is adapted from one by *Bloom* [1967].

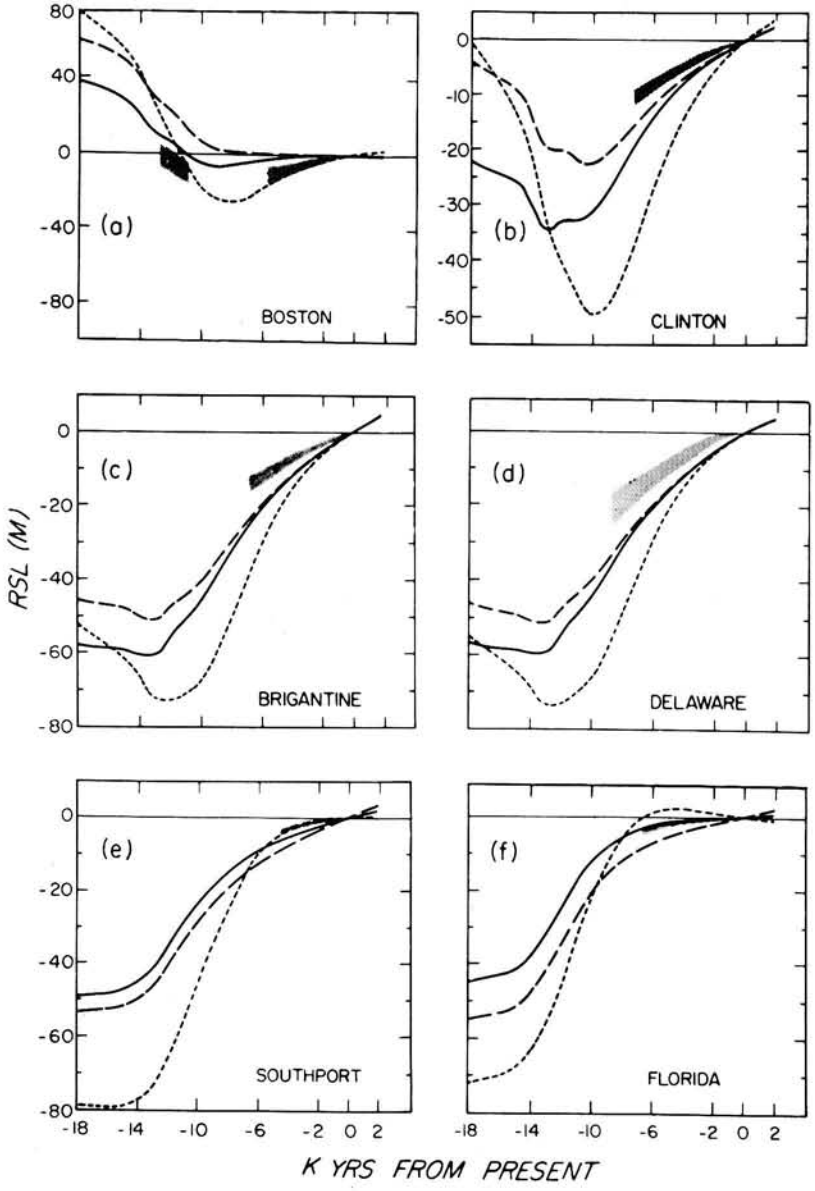

Fig. 3. Observed and predicted RSL histories at six sites along the U.S. East Coast. The observations are denoted by the hatched regions, and the theoretical predictions are for models that differ from one another only in their lower-mantle viscosities. Lithospheric thickness is fixed at $L = 120.7$ km, upper-mantle viscosity at $\nu = 10^{21}$ Pa s, and the short-dashed, long-dashed, and solid curves are the predictions for models that have lower-mantle viscosities ν_{LM} of 10^{21}, 10^{22}, and 5×10^{22} Pa s, respectively. This figure is based upon calculations previously reported by *Wu and Peltier* [1983].

imply that Walcott's inference of LC could be substantially in error.

In this paper I will describe analyses of two different kinds of glacial isostatic adjustment data, one local and the other global, both of which appear quite strongly to require LC $\simeq$ 200 km. The first set of data consists of relative sea level histories from the eastern seaboard of the continental United States, while the second consists of polar wander observations for the past 75 years collected by the International Latitude Service (ILS). In the next section of this paper a detailed discussion is provided of the relative sea level record for sites south of the city of Boston along the U.S. East Coast. The observations are compared with the predictions of a theoretical model that has a fixed lithospheric thickness of 120 km (i.e., the value preferred by McConnell, Sclater, Walcott, and others). These comparisons establish that there are large differences between theory and observation and that these vary systematically from north to south along the coast, suggesting that some property of the model has been incorrectly specified. Attempts are described to remove the systematic error by varying the sublithospheric viscosity profile, but such attempts fail. In section 3 of the paper it is shown that the systematic error may be entirely removed if the lithospheric thickness is simply increased to a value somewhat in excess of 200 km. Section 4 provides an analysis of the secular drift of the rotation pole that is evident in the ILS path, which shows that this observation may also be fit by the isostatic adjustment model but only if the continental lithospheric thickness implied by the data is on the order of 200 km. The two kinds of data are therefore in reasonable agreement in requiring a large value of LC with implications that are discussed in the concluding section 5.

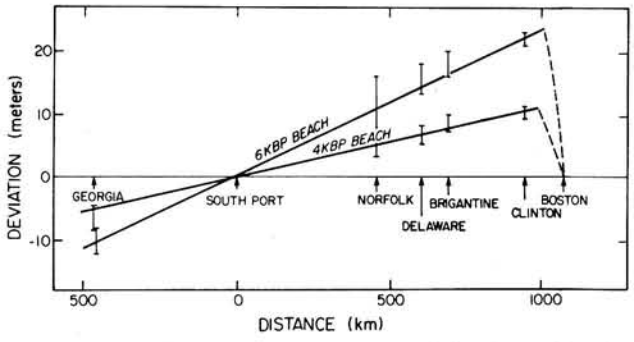

Fig. 4. Deviation of observed and predicted elevations of beaches of age 4000 and 6000 years as a function of distance along the U.S. East Coast measured from Southport. The theoretical predictions employed are those for the model with a constant mantle viscosity of 10^{21} Pa s and 1066B elastic structure.

2. Relative Sea Level Histories

The location map in Figure 1 shows the geographic region with which we will be concerned in this section, the eastern seaboard of the continental United States. This region is particularly important for our purposes because it extends from the location of the ice margin at glacial maximum. The location of the margin is clearly indicated on the figure and passes roughly through the cities of Boston and New York with a northeasterly-southwesterly orientation. Many of the coastal features in this region such as Long Island, Martha's Vineyard Island, Cape Cod, etc., are simply debris from the terminal moraines of this section of the Laurentide ice sheet. For the most part, and for reasons that will shortly become clear, we will here focus on coastal locations from Massachusetts south to Florida, and our interest will be in the history of sea level fluctuations at such locations during the thousands of years that have passed since the disintegration of the Laurentian ice sheet.

Observations of sea level are much more difficult to make in this region than they are at sites that were once under the ice sheet, for the simple reason that relict beaches are drowned rather than raised. The explanation of this is straightforward dynamically. At glacial maximum the weight of the ice depresses the earth's surface beneath it, and the material from the depression is squeezed out into the immediately peripheral region where the land is elevated. After ice sheet disintegration, this deformation is reversed through the process of isostatic adjustment. Sites that were once ice covered are continuously elevated out of the sea by the viscous inflow of material from the peripheral region. Beaches are successively cut into the land as it rises and may be dated using the ^{14}C method. As material flows out of the peripheral region, the surface here sinks below sea level, and the oldest beaches are thus found at the greatest depth below the present level of the sea. The fact that the East Coast of America is presently submerging explains many of the unique properties of its nearshore environment, for example, the extensive occurrence of salt marshes. In order to reconstruct local histories of the variation of sea level from this "drowned" coastal region, one is clearly forced to dredge for old beach material, and particular care must be taken to ensure that such material is in situ [e.g., *Bloom*, 1967]. Clearly, there are a number of nearshore erosional processes that are quite capable, in principle, of vertically displacing such material and thereby obscuring the sea level record.

A summary of several relative sea level (RSL) histories from the region is given in Figure 2, which is modified from *Bloom* [1967]. All of the sea level histories illustrated here show that submergence has been continuous over the past 10–12 kyr. The amounts of submergence have been generally less than 10 m during the past 6 kyr, which contrasts with the amounts of emergence that have been realized over the same time period at sites within the ice margin where uplifts in excess of 100 m are the rule. Of greatest importance for present purposes is the observation from Figure 2 that there does not appear to be a marked systematic variation of the sea level histories as one moves from south to north along the coast. All that can be inferred is that the amount of submergence appears to be less at the southern terminus of the region, Florida, than it is in the north. One might be tempted to ascribe a large fraction of the variation to error in the data and perhaps even to despair that any theoretical use could be made of them. As we will show in what follows, this initial reaction is unwarranted.

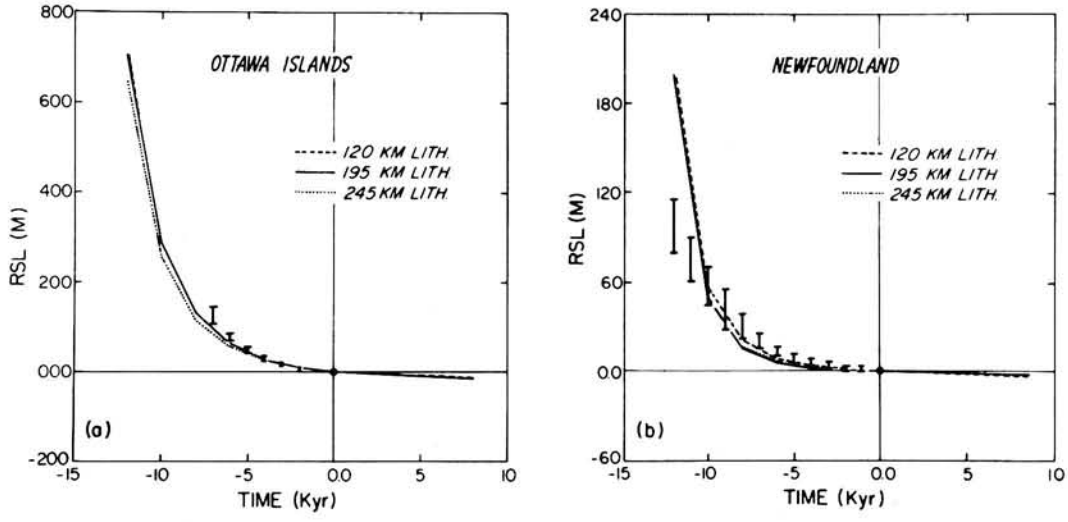

Fig. 5. Comparison of predicted and observed RSL histories at two interior sites: (*a*) Ottawa Islands and (*b*) Northwest Newfoundland, based upon the disk load theory. The dashed, solid, and dotted curves are predictions for models that have lithospheric thicknesses of 120, 195, and 245 km, respectively.

2.1. *Comparisons of Predicted and Observed RSL*

In order to make sense of the above-described observations we require a theoretical model that is capable of predicting RSL histories accurately. Such a model has been developed over the past decade in a sequence of articles that began with *Peltier* [1974]. This paper was devoted to an analysis that showed how one could describe the complete viscoelastic response of the planet to gravitational interaction with a surface mass load. This theory was subsequently extended by *Peltier* [1976], who showed how the viscous part of the response could be described using a normal mode formalism. *Peltier and Andrews* [1976] applied the theory to the explanation of a global set of RSL histories subject to the approximation that the rise of sea level over the global ocean produced by ice sheet disintegration was uniform. *Farrell and Clark* [1976] showed how this approximation could be relaxed to include the self-gravitation of the oceans, and a preliminary sequence of comparisons of the full theory with observations was given by *Clark et al.* [1978] using the numerical methods discussed in detail by *Peltier et al.* [1978]. The theory has now been employed to describe many deglaciation effects other than RSL variations, including free air gravity anomalies [*Peltier*, 1981*b*, 1982; *Peltier and Wu*, 1982; *Wu and Peltier*, 1983] and the observed nontidal acceleration of planetary rotation [*Sabadini and Peltier*, 1981; *Peltier*, 1982, 1983; *Peltier and Wu*, 1983].

In this theory the prediction of relative sea level $S(\theta, \phi; t)$ is obtained as a solution of the following integral equation (see *Wu and Peltier* [1983] for a recent review):

$$S = \rho_i \frac{\phi}{g} *_i L_i + \rho_w S *_0 \frac{\phi}{g} - \frac{1}{A_0} \left\langle \rho_i L_i *_i \frac{\phi}{g} + \rho_w S *_0 \frac{\phi}{g} \right\rangle_0 - \frac{M_i(t)}{\rho_w A_0} \quad (1)$$

in which

$S(\theta, \phi, t)$ relative sea level change;
ρ_i density of ice;
ρ_w density of water;
g surface gravitational acceleration;

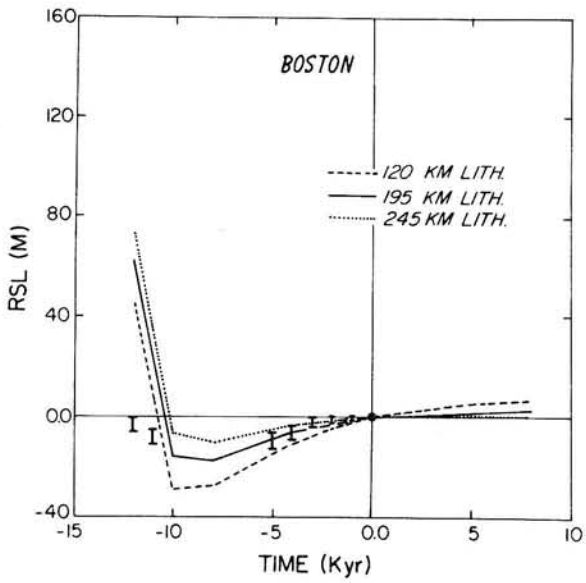

Fig. 6*a*. Same as Figure 5 but for Boston.

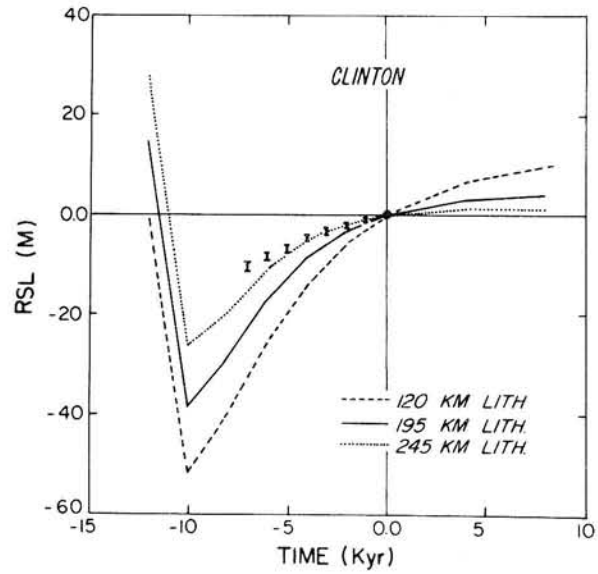

Fig. 6*b*. Same as Figure 5 but for Clinton.

$L_i(\theta, \phi, t)$ mass loss history of the ice sheets;
$\phi'(\theta, \phi, t)$ Green's function for the gravitational potential perturbation forced by a point mass load;
A_0 surface area of the oceans;
$\langle\ \rangle_0$ integral over the surface area of the oceans;
$M_i(t)$ integrated mass loss history of the ice sheets, equal to $-\langle \rho_w S \rangle_0$
$*_i, *_0$ convolutions over the ice sheets and oceans, respectively

Equation (1) is an integral equation because the unknown relative sea level history S appears both on the left-hand side of the equation and under the convolution integrals on the right-hand side. The inputs to the sea level equation are the surface glaciation history $L_i(\theta, \phi, t)$ and Green's function for the gravitational potential perturbation ϕ', which depends upon the radial viscoelastic stratification of the planet. The function $L_i(\theta, \phi, t)$ was first estimated by *Peltier and Andrews* [1976], who provided a tabulation of it called ICE-1. This was refined by *Wu and Peltier* [1983], who call the resulting glaciation history ICE-2 and also present tables of it. The main difference between ICE-2 and ICE-1 is that the new model includes a melting event for Antarctica, although this part of the new glaciation history will not be employed in the sea level calculations discussed here. The second of the functions required to implement the sea level calculation, the impulse response Green's function $\phi'(\theta, \phi, t)$, is calculated using the theory and numerical methods discussed by *Peltier* [1974, 1976] and recently reviewed by *Peltier* [1982] and *Wu and Peltier* [1982].

The earth models employed for the RSL calculations have their elastic structures fixed to that of model 1066B [*Gilbert and Dziewonski*, 1975], which fits a large set of normal mode and body wave seismic data. The steady state shear viscosity of the core is taken equal to zero so that different earth models differ from one another only by virtue of their mantle viscosity profiles and lithospheric thicknesses. The effect of the lithosphere upon the viscoelastic response to surface loading was first discussed with respect to spherical models by *Peltier* [1980]. More detail is given by *Peltier* [1982] and *Wu and Peltier* [1982]. It is important to note that the earth model that is employed to invert the RSL data has no lateral hetero-

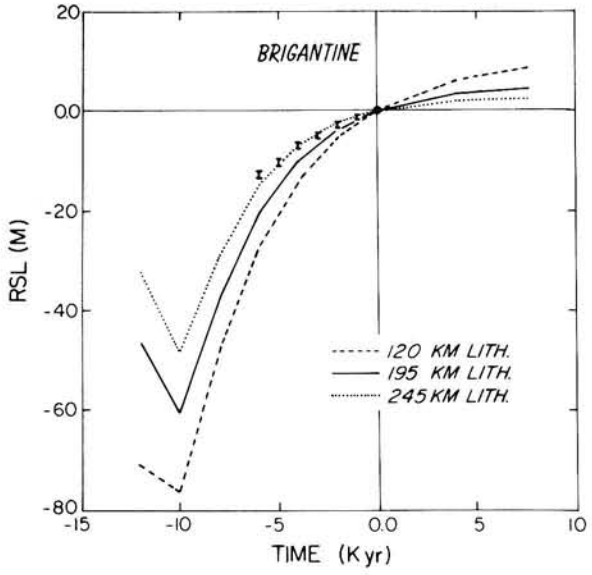

Fig. 6c. Same as Figure 5 but for Brigantine.

geneity. This might be considered a problem insofar as interpreting the RSL data from sites shown in Figure 1 is concerned because these sites are near the boundary between continent and ocean. Clearly, if the RSL data suggest a lithospheric thickness in excess of that appropriate to old ocean floor (~120 km), this is unambiguously attributable to the continental component of the model, particularly so since the continental margin along the U.S. East Coast is especially broad. Once L_i and ϕ' are determined, the sea level equation (1) is solved using a finite element method discussed in detail by *Peltier et al.* [1978].

In Figure 3 we compare observed and predicted RSL histories at six sites along the eastern seaboard of the United States for three different mantle viscosity profiles with the lithospheric thickness held constant at 120 km, that is equal to the value of LC estimated by *Sclater et al.* [1980] on the basis of heat flow data. These results are from calculations described in greater detail by *Wu and Peltier* [1983] but have been collected together in a single new figure motivated by the present application. All earth models have an upper mantle viscosity of 10^{21} Pa s from the base of the lithosphere to the seismic discontinuity at 670-km depth. The short-dashed lines on each plate are the predicted RSL histories for a model whose lower-mantle viscosity ν_{LM} is also 10^{21} Pa s (10^{22} P), the long-dashed lines are for a model with $\nu_{LM} = 10^{22}$ Pa s, and the solid curves are for a model with $\nu_{LM} = 5 \times 10^{22}$ Pa s. Inspection of the individual plates in Figure 3 reveals a rather confusing picture. At Boston the uniform viscosity model is very strongly preferred, since it is the only model that correctly predicts the strongly nonomonotonic RSL history observed at this site. As pointed out by *Peltier* [1974], this behavior is just that expected to be produced by migration of the forebulge, and since such migration is prevented in models that have very high lower-mantle viscosity, such models cannot fit the data. As I have elsewhere argued in detail, the uniform viscosity model is also preferred by RSL data from sites within the ice margin (e.g., around Hudson Bay), but some very modest (approximately $\times 3$) increase of viscosity does seem to be required to fit free air gravity and nontidal acceleration of rotation data [*Peltier and Wu*, 1982, 1983; *Peltier*, 1982, 1983].

As one moves south along the coast from Boston, however, there are large and apparently nonsystematic errors between observation and the predictions of the uniform viscosity model. At Clinton, Brigantine, and Delaware the uniform viscosity model provides the worst of the three model fits to the data, but although an increase of lower-mantle viscosity does reduce the misfits at these sites somewhat, this alteration of the model is not able to remove the misfits completely. At Southport, South Carolina, the situation reverses again, as the data here prefer the uniform viscosity model once more. At this site an increase of lower-mantle viscosity increases the amount of emergence predicted for the past 6 kyr, whereas at the more northern sites this change had reduced the predicted emergence. Moving still further south to Florida in Figure 3*f* we see that the model with highest lower-mantle viscosity is now preferred by the data. The picture presented by this set of comparisons is therefore rather complicated.

Since we know that high lower-mantle viscosity is excluded by RSL data from within the ice margin and also by free air gravity and nontidal acceleration of rotation observations, it is natural to inquire as to whether other conceivable modifications of the mantle viscosity profile, which are not ruled out by such data, might be able to eliminate these misfits. Such attempts were made by *Wu and Peltier* [1983], who discussed them in relation to their Figure 27, and were shown to provide no self-consistent resolution of the problem. It will be useful to establish, however, that there is in fact a highly systematic behavior of the misfits of the predictions of the uniform viscosity model to the observations. If one plots the deviation in meters of the predicted from the observed height of a beach horizon of fixed age as a function of distance along the coast, measured positive north from Southport, then one obtains the result shown in Figure 4. For both the 6- and 4-kyr horizons the misfits between this model and the observations fall on straight lines [*Wu and Peltier*, 1983] for sites south of the city of Boston, the implication being that some simple property of the model has been misspecified. (Note that this misfit falls rapidly to zero at Boston itself, as illustrated in Figure 4.) On the basis of the previously discussed analyses we must suspect that the problem is not with the viscosity of the lower mantle, and the question remains as to what it might be. In what

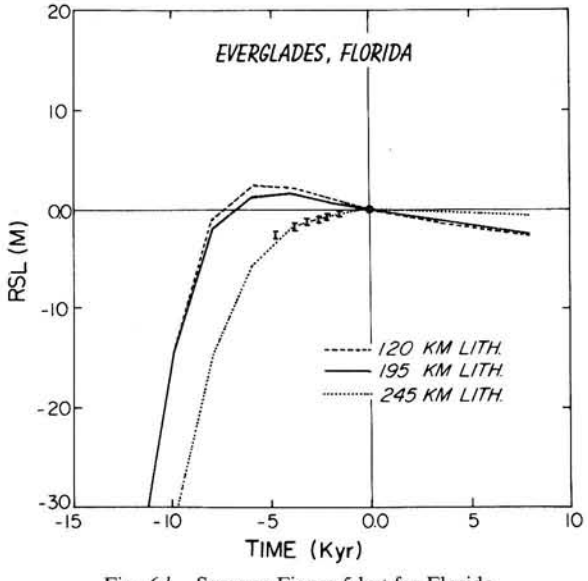

Fig. 6d. Same as Figure 5 but for Florida.

follows, we will discuss a minor adjustment of the model that can solve this problem. First, however, we will introduce a simplified form of the theory, in terms of which this discussion can be more easily pursued.

3. INFLUENCE OF LITHOSPHERIC THICKNESS

Although the comparisons between theory and observation discussed in the last section were all presented within the context of the gravitationally self-consistent model embodied in (1), essentially the same results would have been obtained if these comparisons had been made using a much simpler version of the theory. In this section of the paper we will first establish the validity of this statement and then proceed to exploit the simpler version of the theory to understand the influence on the relative sea level response of variations of lithospheric thickness.

3.1. *Approximate RSL Histories From Radial Displacement Calculations: Theory*

Since the response to surface loading in the near field of an ice sheet is dominated by the direct change in planetary radius forced by glacial unloading and the influence of the water load in the oceans is small in comparison [*Wu and Peltier*, 1983] except for times in excess of ~8 kyr B.P., the latter may be neglected as a first approximation, and the RSL history replaced by the variation of radius. For many purposes we may further simplify the calculation by replacing the actual ice sheet disintegration history by an equivalent disk load approximation. For a circular disk of radius α_0 with center at O we may represent the load per unit area that this ice sheet applies to the earth as $L(\gamma, t)$, where γ is the angular distance from O and t is time. The radial displacement response at a field point Q due to $L(\gamma, t)$ may be calculated by convolution of L with the appropriate space-time Green's function $G(\theta, t)$. If the angular distance $\overline{OQ}$ is equal to θ, then the response $R(\theta, t)$ is

$$R(\theta, t) = \int_{-\infty}^{t} \int_{A} L(\theta', t') G(\gamma', t - t')\, da'\, dt' \qquad (2)$$

where γ' is the angular distance between Q and the element of surface area da' and A is the total area covered by the ice sheet. Now the impulse response Green's function $G(\gamma, t)$ has the normal mode expansion [*Peltier*, 1976]

$$G(\theta, t) = G^E(\theta)\delta(t) + \sum_n \sum_j r_j^n \exp(-s_j^n t) P_n(\cos\theta) \qquad (3)$$

where $G^E(\theta)$ is the elastic contribution to the total response and r_j^n and s_j^n are the initial amplitude and inverse relaxation time of the jth normal mode of viscous gravitational relaxation for the spherical harmonic of nth degree. In writing $G(\theta, t)$ as in (3) we are using a modified form of Green's function for radial displacement. Normally [e.g., *Peltier*, 1976] we write this function as

$$G(\theta, t) = \frac{a}{m_e} \sum_n h_n(t) P_n(\cos\theta) \qquad (4)$$

where a and m_e are the earth's radius and mass, respectively, and where h_n is the surface load Love number, which is usually written

$$h_n(t) = h_n^E \delta(t) + \sum_j q_j^n \exp(-s_j^n t) \qquad (5)$$

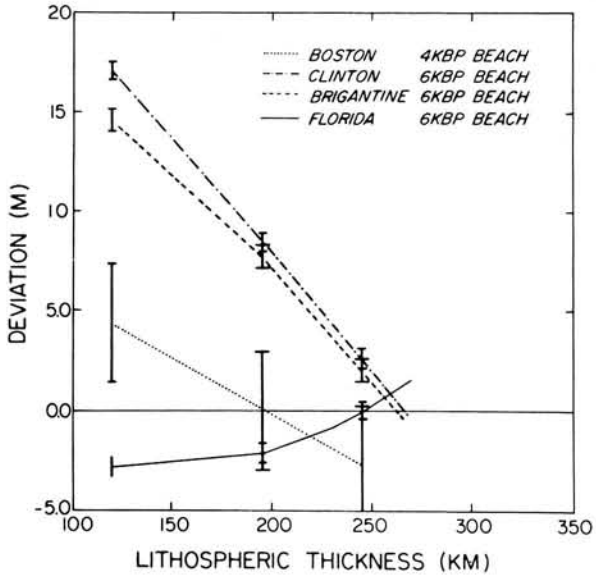

Fig. 7. Deviation of the predicted sea level from the observed as a function of the lithospheric thickness employed in the theoretical model. The variance reduction is illustrated for four of the sites shown in Figure 1. All sites south of Boston agree in requiring a lithospheric thickness near 250 km when the viscosity of the mantle is held constant at the value of 10^{21} Pa s (10^{22} P).

so that

$$G^E(\theta) = \frac{a}{m_e} \sum_n h_n^E P_n(\cos\theta)$$

and

$$r_j^n = \frac{a}{m_e} q_j^n$$

Explicit solutions for the radial displacement response to disk load disintegration histories are provided by *Wu and Peltier* [1983], who obtain a spectral representation for the solution (2) in the form of a simple quadrature for loading histories L, expressible in the form

$$L(\gamma, t) = L_0(\gamma) f(t) \qquad (6)$$

where

$$L_0(\theta) = \rho_I [\alpha\lambda(\alpha_0 - \theta)]^{1/2} \qquad 0 \le \theta \le \alpha_0 \qquad (7)$$
$$L_0(\theta) = 0 \qquad \theta > \alpha_0$$

is assumed for the profile of ice thickness, as is consistent with the assumption that the ice sheet is perfectly plastic in its material behavior. The parameter ρ_I in (7) is the density of ice, and λ is taken to give a maximum thickness of 3500 m with $\alpha_0 = 15°$, which fits the observed maximum form of the Laurentian ice sheet reasonably well.

Although the influence of the fluctuation of ice sheet volume through time is not terribly important at sites within the ice sheet margin [*Wu and Peltier*, 1982], it could conceivably be more important at sites near the margin itself. Accordingly, we shall approximate the time dependence $f(t)$ on the basis of oxygen isotope data taken from deep-sea sedimentary cores. *Broecker and Van Donk* [1970] showed that the ratio $^{18}O/^{16}O$ as a function of depth in deep-sea sedimentary cores, which is direct proxy for the time variation of continental ice volume [*Shackleton*, 1967], was characterized by a slow buildup of the

TABLE 1. Observed and Predicted RSL at Selected Eastern Seaboard Sites

Time, kyr	Southport, m		Virginia, m		New York, m		Brigantine, m		Clinton, m		Boston, m	
	Observed	Predicted	Observed	Predicted	Observed	Predicted	Observed	Predicted	Observed	Predicted	Observed	Predicted
−8	—		−22.0 ± 4.0	−29.52	−17.8 ± 3.0	−22.48						
−7	—		−17.0 ± 3.0	−21.70	−16.0 ± 2.4	−19.06			−10.2 ± 0.7	−20.39		
−6	—		−13.0 ± 3.0	−14.90	−13.0 ± 2.2	−14.45			−8.4 ± 0.5	−15.5		
−5	—		−10.0 ± 3.0	−9.63	−9.4 ± 1.5	−10.02	−10.5 ± 0.6	−11.32	−6.7 ± 0.5	−10.84	−9.0 ± 3.0	−9.02
−4	−3.3 ± 0.5	−2.26	−7.0 ± 1.5	−5.95	−6.40 ± 0.6	−6.56	−7.5 ± 0.5	−7.79	−4.7 ± 0.5	−7.16	−6.0 ± 3.0	−6.03
−3	−2.2 ± 0.4	−0.96	−3.0 ± 1.0	−3.45	−4.4 ± 0.5	−4.00	−5.2 ± 0.5	−4.40	−3.4 ± 0.5	−4.41	−2.5 ± 2.0	−3.74
−2	−1.2 ± 0.2	−0.30	−0.5 ± 0.5	−1.78	−1.2 ± 0.3	−0.88	−3.0 ± 0.4	−2.36	−1.0 ± 0.2	−0.94	−0.5 ± 0.5	−0.84
−1	−0.5 ± 0.1	−0.03	−0.4 ± 0.5	−0.68			−1.4 ± 0.4	−0.95				
0	0	0	0	0	0	0	0	0	0	0	0	0

Calculations are based upon the gravitationally self-consistent model with realistic ICE-2 melting chronology and an earth model with a lithospheric thickness of 245 km and 1066B elastic structure.

main ice complexes over a period of about 9×10^4 years, followed by a fast retreat lasting about 10^4 years. During the last 10^6 years, this 10^5-year cyclic fluctuation of ice volume has been a rather durable feature of the climatic system [e.g., *Hays et al.*, 1976]. On this basis we might expect that a reasonable approximation to $f(t)$ would be

$$f(t) = \frac{t + k\Delta t}{\Delta t} \qquad -k\Delta t \le t \le -(k-1)\Delta t \tag{8}$$

with $\Delta t = 10^5$ years. For the sake of simplicity, we will assume, as in *Wu and Peltier* [1982], that there have been $N = 20$ such cycles since the ice age began (in fact, $N = 10$ would be a better approximation, but the differences are not significant).

3.2. *Approximate RSL Histories From Radial Displacement Calculations: Comparison With Observations*

In Figures 5*a* and 5*b* we compare observed and predicted RSL histories at two sites: the Ottawa Islands in Hudson Bay and a site in northwest Newfoundland. The former location is assumed to correspond to the center of the disk model load, while the latter is assumed to correspond to a location which is 2° inside the ice margin at glacial maximum. These calculations are for earth models with a constant mantle viscosity of 10^{21} Pa s, 1066B elastic structure, but variable lithospheric thickness. The last of the instantaneous model deglaciation events is assumed to have occurred at 11 kyr B.P. in all of these calculations. Computations are shown for three values of lithospheric thickness (120, 195, and 245 km) and inspection of the figure shows that the data are insensitive to the value of LC at the central location and only slightly sensitive at the site just inside the ice margin. This justifies the remark made in the introductory section of this paper to the effect that RSL data from interior points could not be employed to constrain LC for a load of Laurentide scale.

As we move across the ice sheet margin, however, the sensitivity of the predicted response to variations of LC increases dramatically. Figures 6*a*–6*d* compare the model predictions with observations for Boston, Clinton, Brigantine, and Florida, which are, respectively, assumed to be 15°, 16°, 18°, and 27° distant from the disk center. Results are again shown for models that have lithospheric thickness of 120, 195, and 245 km and that are identical to one another in all other respects. Inspection of these figures shows that at all sites south of Boston the model with the greatest lithospheric thickness entirely removes the discrepancy between prediction and observation. At Clinton and Brigantine, increasing the thickness of the lithosphere sharply reduces the net submergence predicted over the past 6 kyr since the end of deglaciation. The thick lithosphere model is somewhat less satisfactory at Boston itself, but since this site is almost exactly on the ice margin, the prediction is very sensitive to slight changes in location with respect to the edge of the disk load, and the misfits cannot therefore be regarded as serious. A summary of the extent of the variance reduction effected by increasing the lithospheric thickness of the model is provided by Figure 7, which shows the way in which the misfit at each site is reduced as LC is increased. The misfits at each of these locations for LC = 120 km may be directly compared with those found from the gravitationally self-consistent calculations that were shown previously in Figure 4. Since the simple disk model results agree very closely with those from the much more complicated model, we should have no doubt that incorporation of the

thick lithosphere into the complete sea level calculation will equally well rectify the misfits originally revealed with it. This is explicitly demonstrated by the data shown in Table 1, in which observed RSL variations at six East Coast sites are compared directly with the predictions of the same gravitationally self-consistent model embodied in (1) as was employed to reveal the misfits originally. For the purpose of these calculations a lithospheric thickness of 245 km was employed. Inspection of the data in this table shows that the variance reduction effected by the increased lithospheric thickness is very similar to that obtained with the simple model. The fact that this single alteration of the radial viscoelastic structure of the earth model at once removes the discrepancy between theory and observation at all sites along the U.S. East Coast is rather strong circumstantial evidence that the thickness of the continental lithosphere must be somewhat in excess of 200 km. In the next section we will briefly discuss a second observational datum that appears to require a value for LC that is of the same order.

4. Lithospheric Thickness From Polar Wander Observations

The second observational datum that will concern us is obtained from the data set illustrated in Figure 8. This shows the variation of the location of the earth's pole of rotation as a function of time over the past 75 years relative to the surface geography. The polar motion is separated into x and y components relative to coordinate axes shown on the inset polar projection with origin at the conventional international origin (CIO). The figure is based on data collected by the ILS [*Vincente and Yumi*, 1969]. Most obvious on this figure is the periodic oscillation whose amplitude variations exhibit a

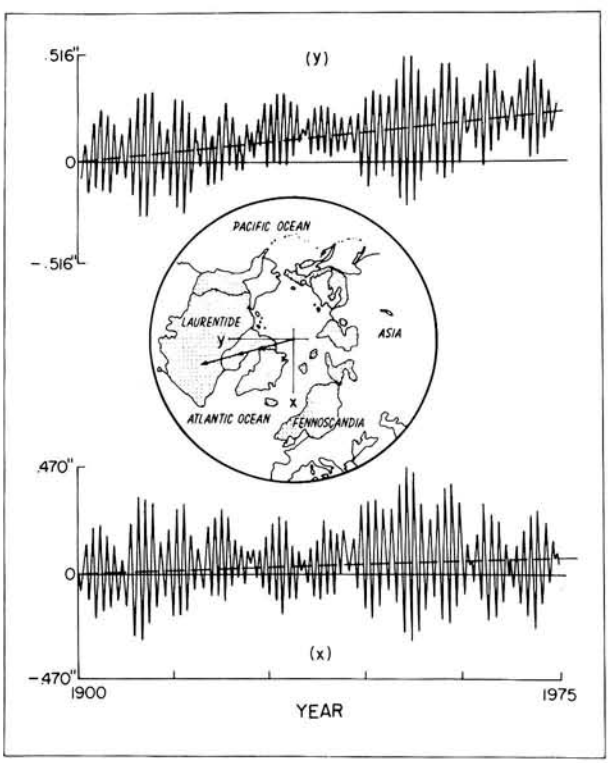

Fig. 8. Polar motion record from A.D. 1900 showing the location of the pole relative to the Conventional International Origin along the x and y coordinate direction shown on the inset polar projection. The locations of the main Pleistocene ice sheets at glacial maximum are indicated by the stippled regions.

TABLE 2. Inertia Perturbations $I_{j3}{}^R$ With Realistic Oceans and Circular Ice Sheets

	$I_{13}{}^R$, kg m^2	$I_{23}{}^R$, kg m^2
Laurentia only (L)	1.203×10^{31}	3.491×10^{32}
Fennoscandia only (F)	-7.504×10^{31}	-3.227×10^{31}
Antarctica only (A)	4.211×10^{30}	5.370×10^{30}
L + F	-6.301×10^{31}	3.168×10^{32}
L + F + A	-5.880×10^{31}	3.222×10^{32}

characteristic beat period that is very close to 7 years. This is due to the superposition of earth's free Eulerian nutation (Chandler wobble), whose period is near 14 months, and the forced annual wobble, whose period is 12 months. The observation that concerns us here, however, is the slow secular drift of the pole upon which the dominant oscillatory disturbance is superimposed. The direction of this drift is as shown by the arrow on the inset polar projection, and the drift rate is 0.95 ± 0.15 deg/10^6 years [e.g., *Dickman*, 1977]. Because the direction of drift is very nearly toward the centroid of the ancient Laurentide ice sheet, we should not be too surprised to learn that this slow polar wander is a memory of the planet of the last deglaciation event of the current ice age. We should furthermore expect that the observed drift rate might be employed to constrain the viscoelastic stratification of the earth's mantle.

That these data might be employed to this effect is an idea that was developed at length by *Peltier* [1982] and *Peltier and Wu* [1983], whose theoretical analysis reveals the existence of serious flaws in prior attempts to employ these data for this purpose [*Nakiboglu and Lambeck*, 1980; *Sabadini and Peltier*, 1981]. The new theory shows that the predicted speed of polar wander depends not only upon the viscosity of the mantle but also upon the magnitude of the lithospheric thickness as well as other characteristics of the viscoelastic stratification. A very brief discussion of the implications of the data insofar as lithospheric thickness is concerned was recently provided by *Peltier and Wu* [1983]. Because of the extensive discussion to be found in these papers and by *Wu and Peltier* [1984], we will not attempt to provide a similarly complete discussion here but rather will simply summarize the results and add some new information to that which has already appeared.

The theoretical analysis presented in the above-cited papers leads to a predicted speed of polar wander in response to the Pleistocene glacial cycle, which takes the form

$$\dot{m}_j(t) = \frac{\Omega}{A\sigma_0} I_{j3}{}^R \left(D_1 \dot{f}(t) + D_2 f(t) + \sum_{i=1}^{N-1} E_i \frac{d}{dt} (f * e^{-\lambda_i t}) \right) \tag{9}$$

in which

$$D_1 = l_s - \sum_{j=1}^{N} \frac{r_j}{s_j} \tag{10a}$$

$$D_2 = -l_s q(0) \Big/ \prod_{i=1}^{N-1} \lambda_i \tag{10b}$$

$$E_i = \left(\frac{l_s q(-\lambda_i)}{\lambda_i} + \sum_{j=1}^{N} \frac{r_j R_j(-\lambda_i)}{s_j} \right) \Big/ \prod_{k \neq i}^{N-1} (\lambda_k - \lambda_i) \tag{10c}$$

The functions $q(s)$ and $R_j(s)$ that appear in (10) are defined as

$$q(s) = s \prod_{i=1}^{N-1} (s + \lambda_i) - \prod_{i=1}^{N} (s + s_i)$$

$$R_j(s) = \prod_{i=1}^{N-1} (s + \lambda_i) - \prod_{i \neq j} (s + s_j)$$

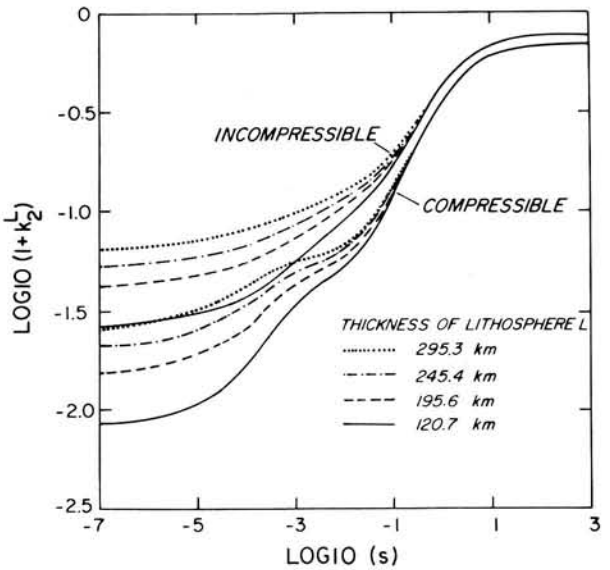

Fig. 9. Plot of the function $1 + k_2{}^L(s)$ as a function of the Laplace transform variable s for models with lithospheric thicknesses of $L = 0$ km (short-dashed curve), $L = 120$ km (long-dashed curve), $L = 195$ km (dash-dotted curve), and $L = 294$ km (solid curve). Since the isostatic factor $l_s = \lim\ (s \to 0)\ [1 + k_2{}^L(s)]$, the divergence of these curves at small s indicates the increase of l_s with L discussed in the text. Plots are shown for both compressible and incompressible models, which are otherwise identical.

and the λ_i are the roots of the degrees $N - 1$ polynomial,

$$Q_N - 1(s) = \sum_j g_j \left[\prod_{i \neq j} (s + s_i) \right] = \prod_{i=1}^{N-1} (s + \lambda_i) \qquad (11)$$

where

$$g_j = (t_j/s_j) \Big/ \sum_{i=1}^{N} (t_i/s_i) \qquad (12)$$

and N is the number of modes of viscous gravitational relaxation required to describe the time domain response to point forcing of the surface load and tidal Love numbers of degree 2. The r_j and t_j are the initial amplitudes of these modes in the surface load and tidal Love numbers, $k_2{}^L$ and $k_2{}^T$, respectively. These Love numbers have the following explicit Laplace transform domain forms:

$$k_2{}^L(s) = (-1 + l_s) - s \sum_{j=1}^{N} \frac{(r_j/s_j)}{(s + s_j)} \qquad (13)$$

$$k_2{}^T(s) = k_f - s \sum_{j=1}^{N} \frac{(t_j/s_j)}{(s + s_j)} \qquad (14)$$

The factor l_s in (13) is called the isostatic factor by *Munk and MacDonald* [1960] and is extremely important for present purposes, as will become clear momentarily. Its value is determined almost exclusively by the thickness of the lithosphere, and so it is partly through this factor that LC influences the rotational response to deglaciation. The parameter k_f in (14) is called the fluid Love number [e.g., *Munk and MacDonald*, 1960] and is the value toward which $k_2{}^T$ tends in the limit of long time (i.e., as $s \to 0$). It may be estimated astronomically from the hydrostatic flattening, which gives $k_f \simeq 0.934$ [e.g., *Lambeck*, 1980]. Among the remaining parameters in the solution (9) are the rotation rate Ω, the equatorial moment of inertia A, and the Chandler wobble frequency of the deformable earth σ_0. The numbers $I_{j3}{}^R$ $(j = 1, 2)$ are the perturbations of the inertia tensor that would be produced by the surface ice and water loads if the earth were rigid, and the function $f(t)$ describes the glacial chronology (the same function as appears in (6)). The inertia perturbations produced by models with realistic oceans and circular ice cap approximations to the major ice sheets are listed in Table 2. For the purposes of the calculations to be discussed here, the ocean basins have been assumed to fill uniformly as the ice sheets melt and to be described by the ocean function [*Balmino et al.*, 1973]. This is a good approximation as evidenced by the exact calculations described by *Wu and Peltier* [1983]. The $f(t)$ we will assume in these calculations is a modified version of (8), which includes a deglaciation phase with a finite duration of 10^4 years that is linear in time, so that the glaciation phase lasts 9×10^4 years, and the duration of individual glaciation pulses remains 10^5 years.

Inspection of the form of the solution (9), in which $\dot{m}_j = \dot{\omega}_j/\Omega$ gives the component of the polar wander velocity in the j direction, shows that at a time like the present of apparent hiatus in a previously continuous glacial cycle, the functions $f = \dot{f} \equiv 0$. Therefore the polar wander velocity may differ from zero only because of the third term in brackets on the right hand side of (9), which contains the convolution integrals $f * e^{-\lambda_i t}$ and therefore depends upon the history of loading. The expression for the coefficients E_i that appear in (9) is given explicitly in (10*c*), inspection of which reveals a joint dependence of the solution on the lithospheric thickness through l_s and on the mantle viscosity profile through r_i, s_i, and λ_i. The strength of the dependence on lithospheric thickness is shown in Figure 9, where the function $1 + k_2{}^L(s)$ is plotted as a function of s on a log-log scale for several values of the lithospheric thickness L and for both compressible and incompressible earth models that are otherwise identical. Since $l_s = \lim\ (s \to 0)\ [1 + k_2{}^L(s)]$, it is clear that the strong divergence of these curves in the small s limit is a manifestation of the strength of the dependence of l_s upon L. For lithospheric thicknesses of $L = 0$, 120.7, 195.6, and 295.3 km the corresponding values of l_s for the compressible models are, respectively, $l_s = 0$, 0.009, 0.016, and 0.027. All of these computations have been done for an earth model with 1066B elastic structure [*Gilbert and Dziewonski*, 1975], a constant mantle viscosity of 10^{21} Pa s, and an inviscid core. Inspection of this

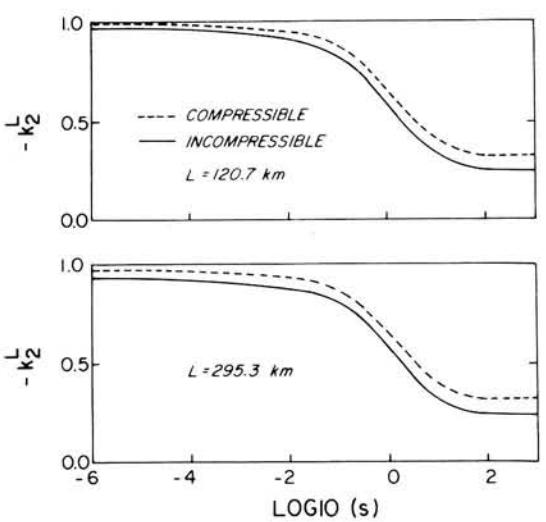

Fig. 10. Plot of the spectral amplitude $-k_2{}^L(s)$ as a function of the Laplace transform variable for models with lithospheric thickness of $L = 120.7$ km and $L = 295.3$ km. Calculations are shown for both elastically compressible and for elastically incompressible models, which are otherwise identical.

figure further shows that the value of l_s is significantly different for an incompressible model (the incompressible equivalent of 1066B) than it is for a compressible model (1066B), a fact that has not previously been pointed out.

For incompressible models the value of l_s for a given lithospheric thickness is significantly greater than for a compressive model that is otherwise identical. Because l_s is a small quantity that is a strong function of L, the logarithmic plot clearly reveals the large differences in the small quantity. Figure 10 plots $k_2{}^L$ itself as a function of the Laplace transform variable s for compressible and incompressible models and for two values of the lithospheric thickness L; s is nondimensionalized with a characteristic time of 10^3 years. This figure provides a reminder of the extent of the distortion of the amplitude spectrum that is produced when one plots $\log_{10}[1 + k_2{}^L(s)]$ as in Figure 9. Figure 11 provides a useful summary of the dependence of l_s upon L for both compressible and incompressible models. For both models $l_s \to 0$ is $L \to 0$. However, for a fixed L the isostatic factor l_s for the incompressible model exceeds that for the compressible model by about 250%. It is therefore clear that if a particular observation requires a particular value of l_s to explain it, one must take the elastic compressibility of the real earth (at least of the lithosphere) into account in the calculation; otherwise one might make a substantial error.

Figure 12 illustrates a sequence of different simplified elastic earth structures for which the solution (2) has been evaluated in detail. They consist of a model with homogeneous elastic properties shown as the dashed lines, a model that has a high-density core but no internal mantle discontinuities (model 1), one which includes the effect of the core and the 670-km discontinuity (model 2), and finally the most complex model, which includes the 420-km discontinuity also (model 3). A complete discussion of the solutions for all of these simple layered models will be found by *Wu and Peltier* [1984]. Here we will focus upon the trade-offs involved between lithospheric thickness L and deep mantle viscosity ν_{LM} for the most complicated of these elastic structures, namely, that labeled 3 on Figure 5. We will assume that the rotational data should be sensitive to the planetary average value of lithospheric

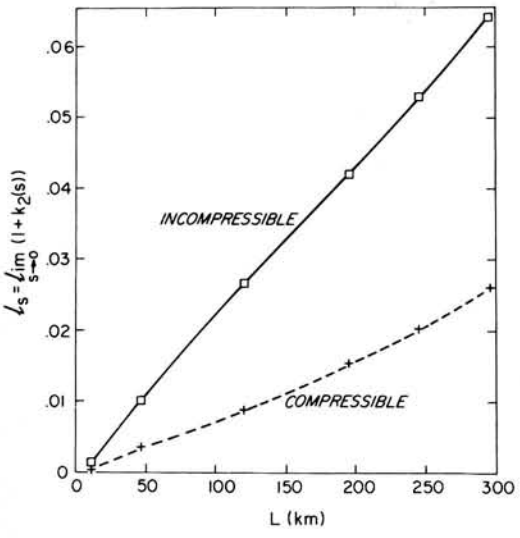

Fig. 11. Plot of the isostatic factor l_s as a function of lithospheric thickness L for both compressible and incompressible models, which are otherwise identical. Note that the isostatic factor for the incompressible model is about 2.5 times larger than that for the compressible model for all values of L.

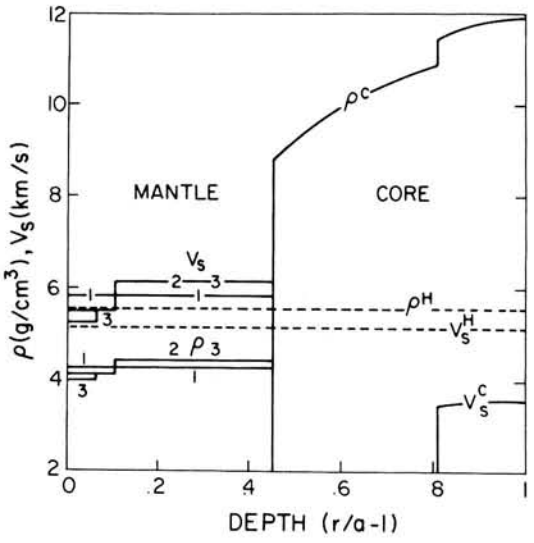

Fig. 12. Elastic properties for a sequence of simplified incompressible earth models. V_s is the shear wave velocity and ρ the density. Only the compressibility of the lithosphere is retained.

thickness $\bar{L} = (2\text{LO} + \text{LC})/3$ and thus that the mean continental thickness will be given by $\text{LC} = 3\bar{L} - 2\text{LO}$, where we have further assumed that the earth's surface is two-thirds oceanic and one-third continental. Some information will also be provided on the sensitivity of the polar wander datum to the presence of internal density discontinuities in the mantle in order to emphasize the high degree of sensitivity that it possesses to all of the characteristics of the internal viscoelastic structure.

Figure 13 shows a plot of the secular determinant (DET) for the degree 2 response, the zeros of which determine the discrete spectrum of N inverse decay times s_i, which are required in the solution (9). Also shown in this figure is the degree $N-1$ polynomial ($\text{POL} = Q_{N-1}$), whose zeros determine the discrete set of $N-1$ associated relaxation times λ_i, which also appear in this solution. Model 3 has nine modes s_i and therefore eight associated inverse relaxation times λ_i. These modes are labeled in Figure 14, which shows their fractional strengths $\beta_j = r_j/s_j/\Sigma r_j/s_j$ for surface load forcing and $g_j = t_j/s_j/\Sigma t_j/s_j$ for tidal forcing. The mode labeling procedure is as by *Peltier* [1976], MO being the (dominant) mode supported by buoyancy across the free outer surface of the model, LO by the lithosphere-mantle interface, CO by buoyancy across the mantle-core interface, and M1–M2 by buoyancy forces across the 670- and 420-km discontinuities, respectively. The modes labeled T1–T4 are transition modes that are not efficiently excited [*Peltier*, 1976]. Inspection of Figure 14 shows that the fractional strengths of the modes for surface load and tidal forcing are significantly different from one another. These differences are such that MO carries a substantially greater fraction of the variance in the tidal spectrum than it does in the surface load spectrum. The greatest difference, however, is in the importance of the M1 mode. It is quite strongly excited by surface load forcing but only very weakly excited by tidal forcing. We note here, as previously, that the presence of the M1 mode is supported by the buoyancy force, which has been assumed in the model to operate across the 670-km discontinuity when it is deflected by an imposed surface or tidal load. Because of the differential sensitivity of this mode to excitation by tidal and surface load forcing and because this differential sensitivity is very important in the solution (9), the observed

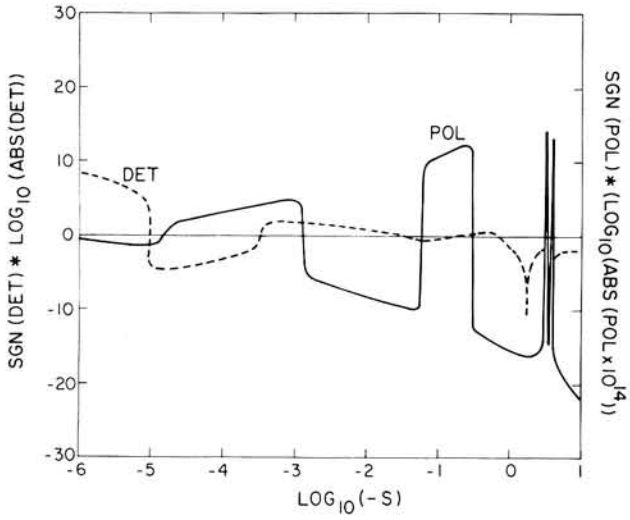

Fig. 13. Plot of the secular function (DET) for elastic model 3 of Figure 15 and of the associated polynomial (POL). The zeros of DET determine the discrete spectrum of N inverse relaxation times s_i, and the zeros of POL determine the discrete spectrum of $N-1$ inverse relaxation times λ_i.

polar wander in the ILS path might eventually prove a useful datum for discriminating as to whether the M1 mode is required in the earth model. A brief discussion of the importance of this effect on the polar wander prediction will be provided below.

Of greatest interest for our present purpose, however, is the result shown in Figure 15*a*, which summarizes the region of LC $-$ ν_{LM} space within which it is possible to fit the polar wander speed obtained from the data shown in Figure 8. In obtaining LC from $\bar{L}$ we have assumed a mean thickness for oceanic lithosphere of 60 km. Any combination of LC and ν_{LM} within the hatched regions will fit the observed speed of 0.95 deg/10^6 years to within the observational error of 0.15 deg/10^6 years. The trade-off calculation has been performed for a single and most plausible choice of the time t' of the observation from the midpoint of the final deglaciation event in the model, and at this time the boundaries of the region in which acceptable solutions exist have been drawn for models assuming seven prior 10^5-year cycles of loading. Further increase of the number of prior cycles from the maximum of seven that we have employed here does not lead to any significant change in the location of the boundaries. Since oxygen isotope data from deep-sea sedimentary cores seem to require t' between the values of 11 and 12 kyr, the model appears to require a value of LC that is near 200 km when the lower-mantle viscosity is fixed to the value near $\nu_{LM} = 3 \times 10^{21}$ Pa s, which is required by recently analyzed Lageos laser ranging data [*Peltier*, 1983]. This value of LC is somewhat smaller than that inferred from the sea level data, but there are several possible explanations of this discrepancy.

One of these is illustrated by the trade-off diagram between $\Delta\rho/\rho$ (670 km) and ν_{LM} shown in Figure 15*b*. The models employed here are of type 2 on Figure 12; that is, they have a single density discontinuity at 670-km depth in the mantle, which is capable of producing a buoyancy force when it is deflected from its equilibrium position by surface loading. The polar wander calculations that delivered the bounds shown on Figure 15*b* employed an earth model with lower-mantle density of $\rho_{LM} = 4372$ kg m^{-3}, while the upper mantle density was varied through the sequence $\rho_{UM} = 4372$, 4300, 4200, and 4100 kg m^{-3} to produce the sequence $\Delta\rho/\rho_{LM} = 0$, 1.65, 3.93, 6.22% of values of the percent change of density in the model at this depth. The sequence of associated elastic shear wave velocities employed was 6117, 5947, 5711, 5475 m s^{-1}. The results of the polar wander speed calculations for this sequence of models (with $\bar{L}$ fixed at 120.7 km) show that the polar wander speed prediction is also sensitive to the presence of any nonadiabatic density variation that may exist at 670-km depth. For fixed ν_{LM} and $\bar{L}$, increasing $\Delta\rho/\rho$ (670 km) increases the predicted speed. Clearly, the lower value of LC implied by the polar wander speed calculations summarized in Figure 15*a* from that implied by the U.S. East Coast RSL data could be increased by decreasing $\Delta\rho/\rho$ (670 km) below the 6.2% used for the models of Figure 15*a*. It is not my purpose here to suggest that this avenue is required, however, but only to point out that the sensitivity of the polar wander datum is such that too much should not be made the discrepancy of the value of LC inferred from it and that suggested by the RLS data. The latter provide by far the more unambiguous estimate of this parameter. A second and more reasonable explanation of the discrepancy between LC inferred flexurally and LC inferred from the rotation data is that not all continental

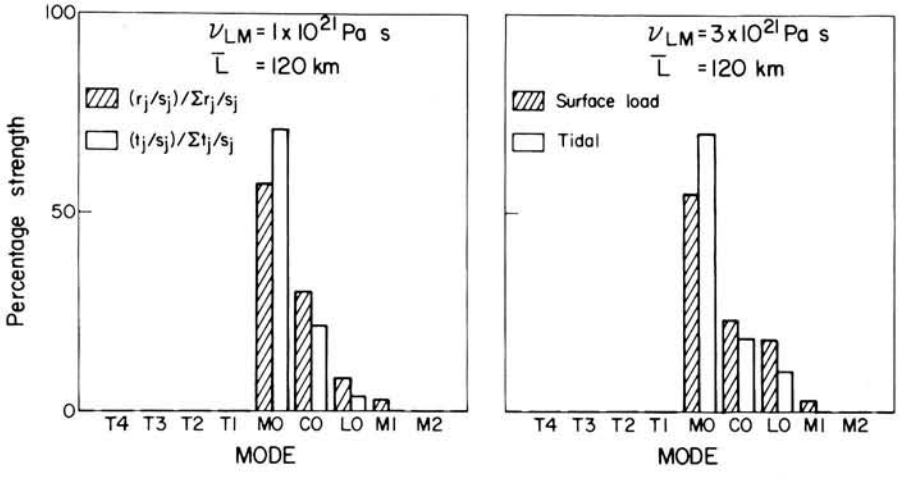

Fig. 14. Fractional strengths for tidal and surface load forcing of the nine modes of viscoelastic relaxation supported by the radially heterogeneous structure of model 3 of Figure 15. The fractional strength denotes the fraction of the total viscous relaxation that is carried by the mode in question; thus the sum of the fractional strengths over all modes equals unity.

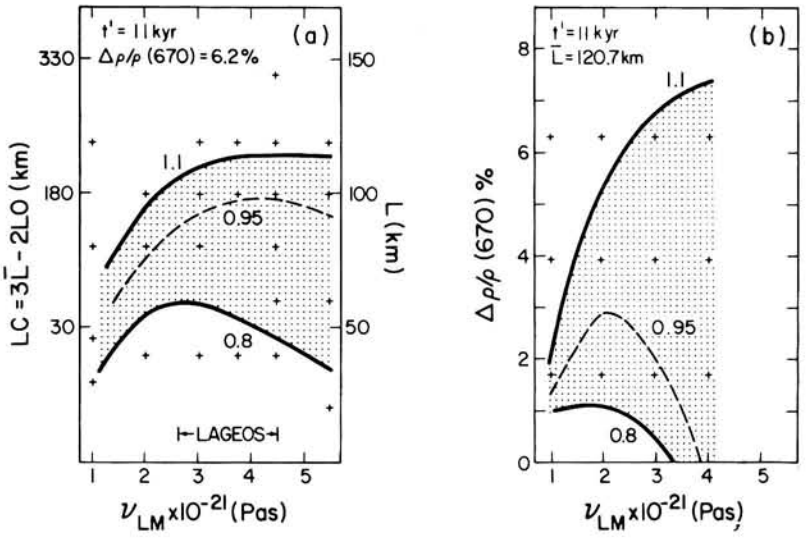

Fig. 15. (*a*) Trade-off between continental lithospheric thickness LC and lower-mantle viscosity ν_{LM} for elastic model 3 of Figure 12. The calculations employ fixed $\Delta\rho/\rho$ (670) = 6.2%, and the predicted polar wander speed is for a time $t' = 11$ kyr following the midpoint of the last model melting event. Any combination of (LC, ν_{LM}) within the two solid boundaries is able to reconcile the observed polar wander speed of 0.95 deg/10^6 years within the observational uncertainty of ± 0.15 deg/10^6 years. (*b*) Trade-off between $\Delta\rho/\rho$ (670) and lower-mantle viscosity ν_{LM} for a sequence of calculations with fixed $\Gamma = 120.7$ km. The solid lines on each plate show the upper and lower bounds (in degrees per million years) the broken lines are for the preferred values of 0.95 deg/10^6 years for the present polar wander speed.

lithosphere has the enhanced thickness inferred from the former method (e.g., the Basin and Range Province of the continental United States).

5. Conclusions

In this paper I have provided a preliminary quantiative analysis of two different sets of geophysical data, both of which appear to require a continental lithospheric thickness near 200 km for their understanding. Although the measurement based upon RLS data is unambiguously associated with the thickness of continental lithosphere, LC, the number obtained from the rotation data is presumably a planetary average value $\bar{L}$. To infer LC from the rotation data, we are obliged to assume that $\bar{L}$ represents a geometric average of LC and LO. Only by assuming that the average oceanic value is known can we then constrain LC with these data. It is interesting that when we employ seismic surface wave data to constrain the average value of LO to a value near 60 km, the rotation data then imply a value of LC that is somewhat lower than that suggested by the RSL data from the East Coast of the United States (i.e., near 200 km compared with the value near 245 km, which was apparently required by the RSL data). Some of this discrepancy can be understood in terms of the trade-off between LC and ν_{LM} in the RSL calculation. The data shown on Figure 3 establish that the modest increase of ν_{LM} required by the Lageos data, from the nominal upper mantle value of 10^{21} Pa s to a value near 3×10^{21} Pa s for ν_{LM}, is such as to allow one to fit the East Coast RSL observations with a somewhat smaller value of LC than the uniform mantle viscosity calculations require. We have also shown in the previous section that the value of LC suggested by the polar wander data would be increased if the nonadiabatic increase of density (or effectively nonadiabatic increase of density) across 670-km depth were considerably smaller than the 6.2% employed for the variable $\bar{L}$ polar wander analyses. A more important bias on the rotationally inferred LC is probably that due to the neglect of regions (like the Basin and Range) where LC is known to be small.

In any event, and on the basis of the arguments presented here, it seems clear that the thickness of the continental lithosphere must be considerably greater than the value of 120 km previously obtained by *McConnell* [1968] and *Walcott* [1970*c*] on the basis of rebound and flexure analysis and reinforced by *Sclater et al.* [1980] using arguments based upon the analysis of heat flow data. On the other hand, our analyses do provide some support for the larger value of continental lithospheric thickness preferred by *Jordan* [1981] on the basis of body wave seismic and petrological data.

The implications of the analysis presented here are varied. If the continental lithospheric thickness is as great as our data appear to require, then there are several different geodynamic models, for example, those for continental collision and for sedimentary basin formation, which will certainly require revision.

Finally, although it is unlikely that the qualitative conclusion reached here, that LC must be much greater than 120 km, will require modification as effort continues, it should be obvious that as yet we have not explored all of the trade-offs involved between allowed variations in the mantle viscosity profile and variations of the lithospheric thickness in the context of different models of the internal elastic structure. These trade-offs are currently being assessed during the course of an analysis of the complete inverse problem for mantle viscosity using the formalism developed by *Peltier* [1976]. In this analysis we are employing all four currently available types of isostatic adjustment data: (1) relative sea level histories, (2) free air gravity anomalies, (3) nontidal acceleration of rotation and $\dot{J}_2$ data, and (4) polar wander constraints. A recent summary of what has been learned through analysis of the forward problems for each of these observations is provided by *Peltier* [1982]. Results from the application of formal inverse theory to the same data will be presented in future publications.

Acknowledgment. I am indebted to Patrick Wu for his assistance with the calculations of section 3.2.

REFERENCES

Balmino, G., L. Lambeck, and W. M. Kaula, A spherical harmonic analysis of the earth's topography, *J. Geophys. Res.*, *78*, 478–481, 1973.

Bloom, A. L., Pleistocene shorelines: A new test of isostasy, *Geol. Soc. Am. Bull.*, *78*, 1477–1493, 1967.

Broecker, W. S., and J. Van Donk, Insolation changes, ice volumes, and the O^{18} record in deep sea cores, *Rev. Geophys. Space Phys.*, *8*, 169–198, 1970.

Canas, J. A., and B. J. Mitchell, Lateral variation of surface wave anelastic attenuation across the Pacific, *Bull. Seismol. Soc. Am.*, *68*, 1637–1650, 1978.

Canas, J. A., B. J. Mitchell, and A. M. Correig, Q_β^{-1} models for the East Pacific Rise and the Nasca plate, in *Mechanisms of Continental Drift and Plate Tectonics*, edited by P. A. Davies and S. K. Runcorn, pp. 123–133, Academic, New York, 1980.

Clark, J. A., W. E. Farrell, and W. R. Peltier, Global changes in postglacial sea level: A numerical calculation, *Quat. Res.*, *9*, 265–287, 1978.

Davies, G. F., and J. W. Strebeck, Old continental geotherms: Constraints on heat production and thickness of continental plates, *Geophys. J. R. Astron. Soc.*, *69*, 623–634, 1982.

Dickman, S. R., Secular trend of the earth's rotation pole: Consideration of motion of the latitude observatories, *Geophys. J. R. Astron. Soc.*, *51*, 229–244, 1977.

Farrell, W. E., and J. A. Clark, On postglacial sea level, *Geophys. J. R. Astron. Soc.*, *46*, 647–667, 1976.

Forsyth, D. W., A new method for the analysis of multi-mode surface wave dispersion: Application to Love wave propagation in the east Pacific, *Bull. Seismol. Soc. Am.*, *65*, 323–342, 1975.

Gilbert, F., and A. Dziewonski, An application of normal mode theory to the retrieval of structural parameters and source mechanisms from seismic spectra, *Philos. Trans. R. Soc., Ser. A*, *276*, 187–269, 1975.

Hays, J. D., J. Imbrie, and N. J. Shackleton, Variations in the earth's orbit: Pace maker of the ice ages, *Science*, *194*, 1121–1132, 1976.

Jarvis, G. T., and W. R. Peltier, Mantle convection as a boundary layer phenomenon, *Geophys. J. R. Astron. Soc.*, *68*, 389–427, 1982.

Jordan, T. H., Continents as a chemical boundary layer, *Philos. Trans. R. Soc. London, Ser. A*, *301*, 359–373, 1981.

Lambeck, K., *The Earth's Variable Rotation: Geophysical Causes and Consequences*, Cambridge University Press, New York, 1980.

McConnell, R. K., Viscosity of the mantle from relaxation time spectra of isostatic adjustment, *J. Geophys. Res.*, *73*, 7089–7105, 1968.

Munk, W. H., and G. J. F. MacDonald, *The Rotation of the Earth*, Cambridge University Press, New York, 1960.

Nakiboglu, S. M., and K. Lambeck, Delgaciation effects on the rotation of the earth, *Geophys. J. R. Astron. Soc.*, *62*, 49–58, 1980.

Oldenburg, D., Conductivity structure of oceanic upper mantle beneath the Pacific ocean, *Geophys. J. R. Astron. Soc.*, *65*, 359–394, 1981.

Parsons, B., and J. G. Sclater, An analysis of the variation of ocean floor bathymetry and heat flow with age, *J. Geophys. Res.*, *82*, 803–827, 1977.

Peltier, W. R., The impulse response of a Maxwell Earth, *Rev. Geophys. Space Phys.*, *12*, 649–669, 1974.

Peltier, W. R., Glacial isostatic adjustment, II, The inverse problem, *Geophys. J. R. Astron. Soc.*, *46*, 669–706, 1976.

Peltier, W. R., Mantle convection and viscosity, in *Physics of the Earth's Interior*, edited by A. Dziewonski and E. Boschi, pp. 362–431, North-Holland, Amsterdam, 1980.

Peltier, W. R., Surface plates and thermal plumes: Separate scales of the mantle convection circulation, in *Evolution of the Earth, Geodynamics Ser.*, vol. 5, edited by R. J. O'Connell and W. S. Fyfe, pp. 229–248, AGU, Washington, D. C., 1981*a*.

Peltier, W. R., Ice age geodynamics, *Annu. Rev. Earth Planet. Sci.*, *9*, 199–225, 1981*b*.

Peltier, W. R., Dynamics of the Ice Age Earth, *Adv. Geophys.*, *24*, 1–146, 1982.

Peltier, W. R., Acceleration in the node of Lageos: A new constraint on deep mantle viscosity, *Nature*, *304*, 434–436, 1983.

Peltier, W. R., and J. T. Andrews, Glacial isostatic adjustment, I, The forward problem, *Geophys. J. R. Astron. Soc.*, *46*, 605–646, 1976.

Peltier, W. R., and J. T. Jarvis, Whole mantle convection and the thermal evolution of the earth, *Phys. Earth Planet Interiors*, *29*, 281–304, 1982.

Peltier, W. R., and P. Wu, Mantle phase transitions and the free air gravity anomalies over Fennoscandia and Laurentia, *Geophys. Res. Lett.*, *9*, 731–734, 1982.

Peltier, W. R., and P. Wu, Continental lithospheric thickness and deglaciation induced true polar wander, *Geophys. Res. Lett.*, *10*, 181–184, 1983.

Peltier, W. R., W. E. Farrell, and J. A. Clark, Glacial isostasy and relative sea level: A global finite element model, *Tectonophysics*, *50*, 81–110, 1978.

Sabadini, R., and W. R. Peltier, Pleistocene deglaciation and the Earth's rotation: Implications for mantle viscosity, *Geophys. J. R. Astron. Soc.*, *66*, 552–578, 1981.

Sauramo, M., Land uplift with hinge lines in Fennoscandia, *Ann. Acad. Sci. Fenn. Ser. A3*, *44*, 1–25, 1958.

Sclater, J. G., C. Jaupart, and D. Galson, The heat flow through the oceanic and continental crust and the heat loss of the earth, *Rev. Geophys. Space Phys.*, *18*, 269–311, 1980.

Shackleton, N. J., Oxygen isotope analysis and Pleistocene temperatures readdressed, *Nature*, *215*, 15–17, 1967.

Vincente, R. O., and S. Yumi, Co-ordinates of the pole (1899–1968), returned to the conventional international origin, *Publ. Int. Latitude Observ. Mizusawa*, *7*, 41–50, 1969.

Walcott, R. I., Flexure of the lithosphere at Hawaii, *Tectonophysics*, *9*, 435–446, 1970*a*.

Walcott, R. I., Isostatic response to loading of the cust in Canada, *Can. J. Earth Sci.*, *7*, 716–727, 1970*b*.

Walcott, R. I., Flexural rigidity, thickness and viscosity of the lithosphere, *J. Geophys. Res.*, *75*, 3941–3954, 1970*c*.

Watts, A. B., and S. F. Daley, Long wavelength gravity and topography anomalies, *Annu. Rev. Earth Planet. Sci.*, *9*, 415–448, 1981.

Wu, P., and W. R. Peltier, Viscous gravitational relaxation, *Geophys. J. R. Astron. Soc.*, *70*, 435–486, 1982.

Wu, P., and W. R. Peltier, Glacial isostatic adjustment and the free air gravity anomaly as a constrain on deep mantle viscosity, *Geophys. J. R. Astron. Soc.*, *74*, 377–450, 1983.

Wu, P., and W. R. Peltier, Pleistocene deglaciation and the earth's rotation: A new analysis, *Geophys. J. R. Astron. Soc.*, *76*, 753–792, 1984.

W. R. Peltier, Department of Physics, University of Toronto, Toronto, Ontario, Canada M5S 1A7.

(Received May 2, 1983;
revised March 23, 1984;
accepted May 8, 1984.)